

## Cationic substitution and role of oxygen in the $n$ -type superconducting $T'$ system $\text{Nd}_{2-y}\text{Ce}_y\text{CuO}_z$

E. Wang, J.-M. Tarascon, L. H. Greene, and G. W. Hull  
Bellcore, 331 Newman Springs Road, Red Bank, New Jersey 07701

W. R. McKinnon  
National Research Council of Canada, Ottawa, Canada K1A 0R9  
(Received 16 August 1989)

The effect of oxygen content and cationic substitution on the structural and superconducting properties of the  $T'$  phase were studied by investigating the  $\text{Nd}_{2-y}\text{Ce}_y\text{CuO}_z$  and  $R_{1.85-x}R'_xM_{0.15}\text{CuO}_z$  ( $R = \text{Nd, Eu}$ ;  $R' = \text{La, Y}$ ;  $M = \text{Ce, Th}$ ;  $z \cong 4$ ) series. We find that solid solutions of the  $T'$  phases can be prepared, and the solubility range of La and Y depends on the sizes of the host versus the dopant ions. The transition from tetragonal  $T'$  phase to the orthorhombic  $T$  phase is quite abrupt, without evidence for the  $T^*$  phase. In this system, as for the La-Sr-Cu-O system, we find that superconductivity seems to correlate with the in-plane Cu-Cu distance, and there is a critical distance (3.95 Å) for which  $T_c$  is maximum. The as-prepared Ce- or Th-doped materials have an oxygen content per unit formula greater than four, and when heated under nitrogen they lose oxygen in two steps at temperatures of 400 and 800°C, with the amount of oxygen lost through each step being strongly dependent on sample processing. The total amount of mobile oxygen lost decreases with increasing Ce or Th content. From thermogravimetric-analysis measurements we show the crucial importance of the reducing step at temperatures greater than 850°C for inducing superconductivity as well as the importance of the cooling rate on the superconducting properties of the  $T'$  phases. The importance of oxygen disorder to the normal-state properties is demonstrated.

### INTRODUCTION

Since the first discovery of high- $T_c$  superconductivity<sup>1</sup> in the  $\text{La}_{2-x}\text{Ba}_x\text{CuO}_4$  system that has a distorted  $\text{K}_2\text{NiF}_4$  structure (or the so-called  $T$  phase), superconductivity has also been found in two other  $\text{K}_2\text{NiF}_4$ -related structures,  $T'$  and  $T^*$  phases (Refs. 2 and 3, respectively). The  $T'$  phase  $R_2\text{CuO}_4$  ( $R = \text{Pr-Gd}$ ) is exhibited by most rare earths, whereas the cuprate  $T$  phase is found only when  $R = \text{La}$ . One major difference between the  $T$  and  $T'$  phases is the coordination of copper. Copper in the  $T$  phase has a sixfold coordination with four of the oxygen atoms in the  $\text{CuO}_2$  plane, and the remaining two oxygen atoms (called apical oxygen) above and below the Cu atoms. In contrast, copper in the  $T'$  phase is in fourfold coordination (i.e., no apical oxygen). Intermediate between the  $T$  and  $T'$  phases is the  $T^*$  phase,  $\text{La}(\text{Pr})_{2-x-y}R_x\text{Sr}(\text{Ba,Ca})_y\text{CuO}_4$  ( $R$  denotes rare earth), in which Cu is fivefold coordination with oxygen atoms occupying both the  $4d$  (apical oxygen) and  $4e$  (fluorite-type oxygen) sites.<sup>4</sup> Here we determine, as a function of the rare earth, the structural stability of the  $T'$  phase with respect to the  $T$  and  $T^*$  phases. We report our studies of the La- and Y-substituted  $R_{1.85}R'_xM_{0.15}\text{CuO}_{4-y}$  ( $R = \text{Nd, Eu}$ ;  $R' = \text{La, Y}$ ;  $M = \text{Ce, Th}$ ) systems.

The superconductors with the  $T^*$  or  $T$  structure are  $p$  type (i.e., the carriers are holes), whereas the superconductors with the  $T'$  structure are  $n$  type (i.e., the carriers are electrons). This difference is indirectly revealed from the way in which superconductivity is induced in these

phases. Superconductivity is induced in the  $T$  and  $T^*$  phases by increasing the oxidation state of Cu either by divalent dopant (e.g., Sr) and/or by means of an oxidizing atmosphere. On the other hand, to promote superconductivity in the  $T'$  phase, it is necessary not only to lower the oxidation state of copper by a tetravalent dopant but also to anneal the as-grown sample in a reducing atmosphere. It is therefore important to determine how oxygen content affects superconductivity behavior in the  $T'$  phase by studying the  $\text{Nd}_{2-y}\text{Ce}_y\text{CuO}_z$  system along with other series in which trivalent Nd ions are replaced partially by La or Y, completely by Eu, or in which the tetravalent Ce ions are replaced by Th.

Finally the  $T^*$  phase, whose unit cell can be viewed as containing half of the unit cell of the  $p$ -type  $T$  phase and half of the unit cell of the  $n$ -type  $T'$  phase, appears as an attractive system in which one could expect, depending on the nature of the chemical doping, to achieve either  $p$ - or  $n$ -type superconductivity. Doping studies on the  $T^*$  phase were performed, and our results will be briefly mentioned here. Fluorine substitution or tetravalent substitution have failed to produce  $n$ -type superconductivity in the  $T^*$  materials.

### EXPERIMENTAL

To simultaneously study the structural stability of the  $T'$  phase with respect to the  $T$  and  $T'$ , as well as its  $T_c$  dependence as a function of the rare earths, we first undertook a survey of several series of samples of general formula  $R_{2-x-y}R'_x\text{Ce}_y\text{CuO}_z$  to determine the Ce content

( $y$ ) at which  $T_c$  is maximum. We found that for a fixed rare-earth  $R/R'$  ratio,  $T_c$  was always maximum for Ce content close to 0.15. Thus, in the following we focused only on the series with  $y=0.15$ . The  $R_{1.85-x}R'_xM_{0.15}CuO_z$  solid solutions were prepared by heating the appropriate oxides in the required stoichiometry in air for 20 h at 900°C with two grindings and making into pellets before annealing at 1100°C for 12 h or longer (step 1). A second annealing at 900°C under  $N_2$  (step 2) was required in order to induce superconductivity in these samples. We found that the superconducting properties of Ce-doped samples are strongly affected by the cooling rate in both synthesis steps 1 and 2, and the annealing temperature in step 2. Unless otherwise stated, the samples were cooled in air from 1100°C in 2 h (step 1), and in nitrogen from 900°C in 4 h (step 2).

Fluorination was carried out on two of the reported  $T^*$  phases, and samples of  $La_{1.08}Dy_{0.72}Sr_{0.2}CuO_{4-x}F_x$  and  $La_{0.84}Sm_{0.96}Sr_{0.2}CuO_{4-x}F_x$  with ( $x=0-0.35$ ) were prepared by heating the corresponding oxides and  $DyF_3$  and  $SmF_3$  at 920°C for 15 h, with one regrinding. The powders were then made into pellets and fired at 1050°C for 18 h in air and annealed in  $N_2$  at 890°C for 12 h.

Oxygen stoichiometry was obtained by thermogravimetric analysis (TGA) measurements under various atmospheres ( $N_2, O_2$  or 4%  $H_2$  in Ar) with a heating rate of 5°C/min. X-ray-diffraction measurements with Cu  $K\alpha$  radiation were used to determine the range of existence of the solid solutions. The upper limit of solubility range was taken as the highest value of  $x$  ( $R'$  content) or  $y$  (Ce or Th content) for which the samples did not show a trace of the second phase. Lattice parameters for single-phase materials were refined using the Bragg peaks over the  $\theta$  range,  $20^\circ < 2\theta < 80^\circ$ , as described in Ref. 8. Superconductivity transition temperatures were determined by ac-susceptibility measurements (13 Hz), and the resistivity temperature dependence was measured with a standard four-probe configuration.

## RESULTS

Solid solutions of  $Nd_{2-x}La_xCuO_z$  can be synthesized in the range  $0 < x < 0.9$ . With Ce doping, the range was extended to  $0 < x < 1.2$  in  $Nd_{1.85-x}La_xCe_{0.15}CuO_4$  series [Fig. 1(a)]. Mixtures of  $T$  and  $T'$  phases were found in the range  $1.2 < x < 1.7$  for the  $Nd_{1.85-x}La_xCe_{0.15}CuO_4$  series and in the range  $0.9 < x < 1.65$  for the  $Nd_{2-x}La_xCuO_4$  series. Pure  $T$  phase was formed for  $x > 1.7$  and  $x > 1.65$  for the Nd-La-Ce-Cu-O and Nd-La-Cu-O series, respectively. The transition from tetragonal  $T'$  phase to the orthorhombic  $T$  phase with increasing La doping is quite abrupt (i.e., that the two-phase region is narrow). For both series, no peaks due to the  $T^*$  phase was detected in the powder x-ray diffraction through the two-phase region. This, in conjunction with the recent report<sup>4</sup> on new  $T^*$  phases containing  $Ca^{2+}$ ,  $Ba^{2+}$ , or  $Sr^{2+}$ , indicates that the stability of the  $T^*$  phase is probably more sensitive to alkaline earth than rare-earth dopant. This is also evident from our failure to synthesize  $T'$  phases of  $Nd_{2-x-y}La_xSr_yCuO_4$ . As soon

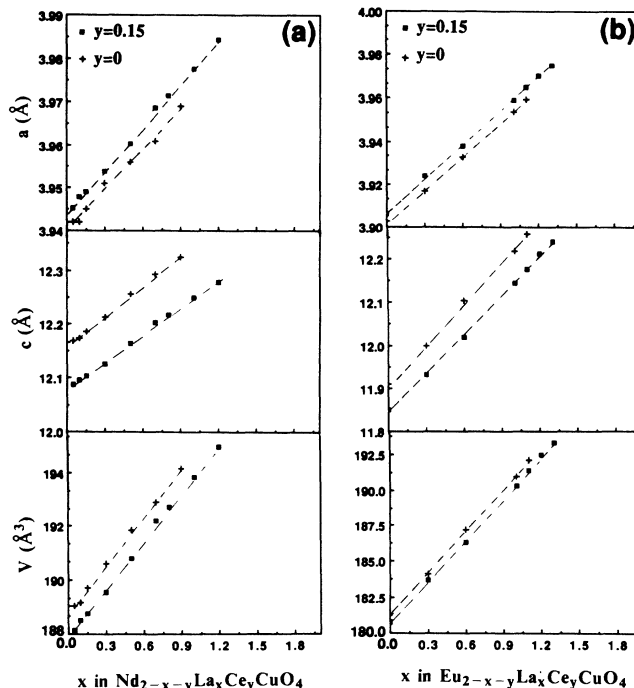


FIG. 1. Variation of the tetragonal lattice parameters  $a, c$  and volume  $V$  as a function of the  $x$  for the (a)  $Nd_{2-x-y}La_xCe_yCuO_4$  series and (b)  $Eu_{2-x-y}La_xCe_yCuO_4$  series.

as Sr doping is introduced, mixtures of  $T'$  and  $T^*$  phases formed.

When Nd was replaced by the smaller Eu ion in  $Eu_{1.85-x}La_xCe_{0.15}CuO_4$ , the solubility range of La increased to  $0 < x < 1.35$  [Fig. 1(b)], and as for the Nd system already described, one finds that the Ce doping extends the solubility range of La. A small decrease in the solubility range of La ( $0 < x < 1.1$  instead of  $0 < x < 1.2$ ) was only observed when Ce was replaced by a Th ion in the  $Nd_{1.85-x}La_xTh_{0.15}CuO_4$  series [Fig. 2(a)]. These solid solutions illustrate the importance of size of the host ( $Nd_2CuO_4$ ) versus the dopant ions (Ce and Th) in stabilizing the  $T'$  phase. When  $Nd^{3+}$  (1.25 Å) is partially substituted by the smaller  $Ce^{4+}$  (1.11 Å) dopant, more  $La^{3+}$  is substituted for  $Nd^{3+}$  in  $Nd_{1.85-x}La_xCe_{0.15}CuO_4$  than in  $Nd_{2-x}La_xCuO_4$ . Similarly, one finds the solubility range of La in  $M_{2-x}La_xCe_{0.15}CuO_4$  to increase when Nd is replaced by a smaller ion,  $Eu^{3+}$  (1.21 Å). In contrast, the size effect is not very pronounced when comparing  $Nd_{1.85-x}La_xCe_{0.15}CuO_4$  [Fig. 1(a)] with  $Nd_{1.85-x}La_xTh_{0.15}CuO_4$  series [Fig. 2(a)]. This is because  $Th^{4+}$  (1.13 Å) and  $Ce^{4+}$  (1.11 Å) have a similar ionic radius.

In the case of the Y-substituted series, one observes that the  $Nd_{1.85-x}Y_xCe_{0.15}CuO_4$  series [Fig. 2(b)] have a smaller solubility than the  $Nd_{1.85-x}La_xCe_{0.15}CuO_4$  series, since  $Y^{3+}$  (1.16 Å) is smaller than  $La^{3+}$  or  $Nd^{3+}$ . Comparison of the  $Nd_{1.85-x}Y_xCe_{0.15}CuO_4$  with  $Nd_{2-x}Y_xCuO_4$  series [Fig. 2(b)] shows that the addition

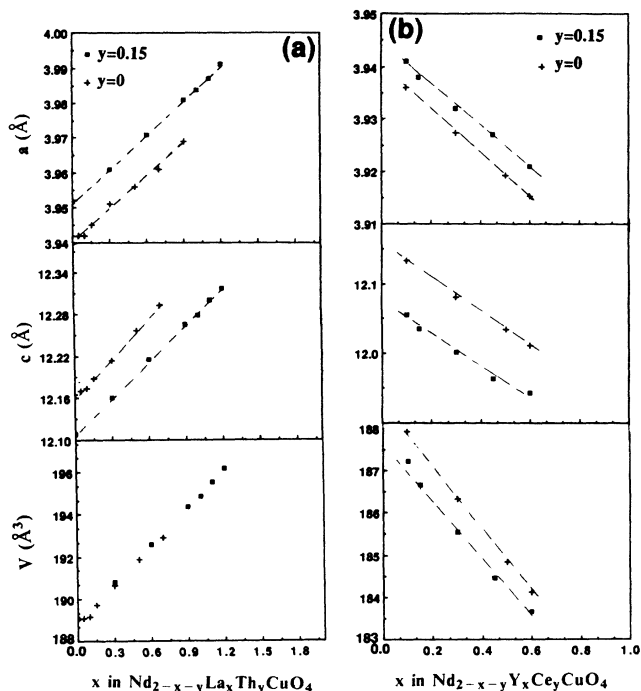


FIG. 2. Variation of the tetragonal lattice parameters  $a$ ,  $c$  and volume  $V$  as a function of the  $x$  for the (a)  $\text{Nd}_{2-x-y}\text{La}_x\text{Th}_y\text{CuO}_4$  series and (b)  $\text{Nd}_{2-x-y}\text{Y}_x\text{Ce}_y\text{CuO}_4$  series.

of Ce does not enhance the Y solubility, in contrast to the La-doped Eu and Nd series. Indeed, the solubility range is about the same for both series, and at large Y concentration peaks due to  $\text{Y}_2\text{Cu}_2\text{O}_5$  were detected by powder x-ray diffraction. Thus, large Y concentrations tend to destabilize the  $T'$  structure and form the  $\text{Y}_2\text{Cu}_2\text{O}_5$  phase, confirming that the  $T'$  or  $T$  phase cannot be synthesized for rare earths with small ionic radii.<sup>5</sup>

In all the La substituted series,  $R_{1.85-x}\text{La}_x\text{M}_{0.15}\text{CuO}_{4-y}$  ( $R = \text{Nd, Eu}$ ;  $M = \text{Ce, Th}$ ), the lattice parameters  $a$ ,  $c$ , and the volume of the tetragonal unit cell increase with increasing La concentration. The opposite was observed for the Y-substituted  $T'$  phases. This is because La is larger than Nd and Eu, whereas Y is smaller than Nd and Eu. A general observation is that independent of the doping element, the  $a$  and  $c$  lattice parameters either increase or decrease simultaneously. In fact the  $a$  and  $c$  parameters for all compounds with a Ce content of 0.15 are almost perfectly correlated, meaning that all compounds with a given  $a$  have the same  $c$  and hence the same volume. As an example,  $a = 3.95 \text{ \AA}$ ,  $c = 12.129 \text{ \AA}$ , and  $V = 189.5 \text{ \AA}^3$  compared to  $a = 3.953 \text{ \AA}$ ,  $c = 12.116 \text{ \AA}$ , and  $V = 189.36 \text{ \AA}^3$  for the  $\text{Nd}_{1.55}\text{La}_{0.3}\text{Ce}_{0.15}\text{CuO}_z$  and  $\text{Eu}_{0.95}\text{La}_{0.9}\text{Ce}_{0.15}\text{CuO}_z$  compounds, respectively. Finally for the as-grown materials and reduced materials, the change in the lattice parameters were very small and in the limit of our resolution.

The superconducting critical temperature were determined for all the members of the Ce- or Th-doped series by the inductive method. In Fig. 3 we plot the  $T_c$ 's

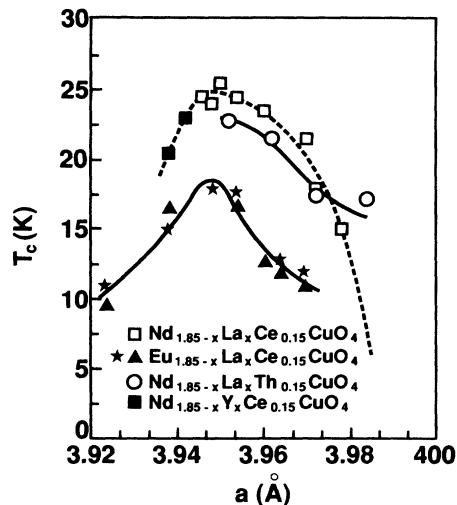


FIG. 3.  $T_c$  (onset) as determined by ac susceptibility vs the  $a$  lattice parameter. For the Eu series, two sets of samples were investigated. Samples represented by the triangles were prepared as described in the text. The samples represented by a star were prepared by removing nitrogen at  $1000^\circ\text{C}$ , putting back oxygen at  $840^\circ\text{C}$ , and removing nitrogen at  $900^\circ\text{C}$

(determined as the onset of the ac signal for quenched samples) as a function of the  $a$  crystallographic distance (i.e., Cu-Cu distance within the  $\text{CuO}_2$  plane). Note a correlation between the lattice parameter  $a$  and the superconducting onset temperatures ( $T_c$ ). The optimum onset temperature ( $T_c = 25 \text{ K}$ ) for the lanthanum Ce-doped samples is found for  $a$  between  $3.945$  and  $3.955 \text{ \AA}$ . A dramatic decrease in  $T_c$  is observed when  $a$  becomes either greater than  $\approx 3.96 \text{ \AA}$  or less than  $\approx 3.94 \text{ \AA}$ . Interestingly, La doping seems to raise the onset of  $T_c$  from  $12.5 \text{ K}$  in  $\text{Eu}_{1.85}\text{Ce}_{0.15}\text{CuO}_4$  ( $a \approx 3.947 \text{ \AA}$ ) to about  $17 \text{ K}$  in  $\text{Eu}_{0.9}\text{La}_{0.9}\text{Ce}_{0.15}\text{CuO}_4$  ( $a \approx 3.953 \text{ \AA}$ ). In the  $\text{Nd}_{1.85-x}\text{Y}_x\text{Ce}_{0.15}\text{CuO}_4$  series, superconductivity was observed only for  $a$  greater than  $\approx 3.94 \text{ \AA}$ . These results show that in the  $T'$  phases there is a very critical and narrow range of  $a$  distances to obtain high  $T_c$ . In support of this correlation, it is worth mentioning that the  $a$  lattice parameter of the highest- $T_c$  fluorine-doped material,<sup>6</sup>  $\text{Nd}_2\text{CuO}_{3.7}\text{F}_{0.3}$  falls also into the maximum of Fig. 3 with  $a \approx 3.945 \text{ \AA}$ .

The temperature dependence of resistivity for the members of each series that showed the highest  $T_c$ 's are shown in Fig. 4. The  $T_c$  values are in good agreement with those deduced from ac-susceptibility measurements. Above  $T_c$ , the resistivity is semiconductinglike, as usually found for polycrystalline ceramics of this system, and explained in terms of composition inhomogeneities.<sup>7</sup> In the  $\text{Nd}_{2-x}\text{La}_x\text{Ce}_{0.15}\text{CuO}_4$  series, with increasing La content beyond  $x = 1$ , one destroys superconductivity and promotes semiconducting behavior. This result contrasts with the superconducting to metallic transition observed for the La-Sr-Cu-O system or Nd-Ce-Cu-O systems upon increasing Ce or Sr content, respectively.<sup>8,9</sup>

Meissner and shielding measurements performed on

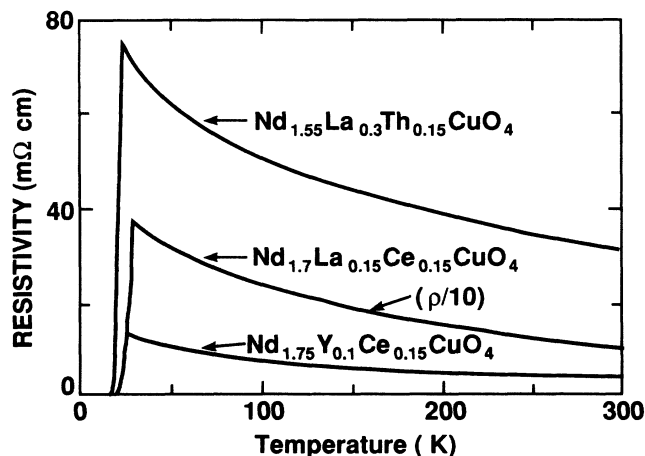


FIG. 4. Temperature-dependent resistivities of selective  $T'$  phase compounds which have shown the highest  $T_c$  by ac-susceptibility measurements.

several members of the Ce-doped Eu and Nd series, by means of a SQUID magnetometer, reveal that the superconducting volume fraction does not exceed 25%. This volume fraction is independent of the cation ratio.

A depression in  $T_c$  by magnetic ions is commonly observed in a conventional superconductor. Since the rare earths are closer to the  $\text{CuO}_2$  plane in the  $T'$  phase than in the  $T$  phase (1.81 Å as compared to 2.41 Å), one would expect a greater sensitivity of  $T_c$  to rare-earth doping in the  $T'$  phase, and thereby the  $T_c$  of Nd compound to be smaller than that of the Eu compound [in which  $\text{Eu}^{+3}$  is a Van Vleck ion ( $J=0$ )]. We note, however, the opposite;  $T_c$  is smaller for the Eu compound than for the Nd compound. Therefore, as for the  $\text{La}_{2-x}\text{M}_x\text{Sr}_{0.2}\text{CuO}_4$  ( $T$ ) system with  $M=\text{La}$  to  $\text{Eu}$ ,<sup>10</sup> we conclude the magnetism is obviously not the explanation for the depression in  $T_c$  observed in the  $T'$  phases when Nd is replaced successively by Pr, Sm, and Eu.<sup>11,12</sup>

Finally, we find that among the  $T^*$  phases investigated, fluorination is only possible within the  $\text{La}_{1.08}\text{Dy}_{0.72}\text{Sr}_{0.2}\text{CuO}_{4-x}\text{F}_x$ , system and single phases are obtained only for values of  $x$  ranging from 0 to 0.35. Refinement of the lattice parameters (Table I) shows a slight contraction of the  $c$  axis and slight expansion of the  $a$  axis, as observed in the  $\text{Nd}_2\text{CuO}_{4-x}\text{F}_x$  series.<sup>6</sup> Independent of the cooling rate or ambient used, none of the fluorinated samples show superconductivity.

## OXYGEN DOPING

In addition to the Ce content, another critical parameters which affects  $T_c$  in the  $T'$  phases ( $\text{Nd}_{2-x}\text{Ce}_x\text{CuO}_z$  or  $\text{R}_{2-x-y}\text{R}'_x\text{Ce}_y\text{CuO}_z$ ) is the oxygen content ( $z$ ). For example, when  $\text{Nd}_{1.85}\text{Ce}_{0.15}\text{CuO}_z$  is annealed in  $\text{N}_2$  below 700°C, no superconductivity is detected. Reannealing the sample at 820°C, a weak and incomplete superconducting transition is observed with a  $T_c$  (onset)  $\cong 16$  K. On further annealing, the sample at 900°C, bulk superconductivity is observed at 24 K. Finally, superconductivity is lost on further annealing at temperatures greater than 1000°C. Thus, we investigated the role of the nitrogen annealing treatment and more precisely how the oxygen stoichiometry affects superconductivity in these compounds by the TGA technique.

The effect of cooling rate on the oxygen content of the as-grown or reduced material was studied on the compound  $\text{Nd}_{1.85}\text{Ce}_{0.15}\text{CuO}_z$ . Two pellets of this compound were annealed at 1100°C for 14 h. Then one pellet (denoted  $Q$ ) was quenched from 1100°C and the other pellet (denoted  $S$ ) was slowly cooled (8 h) to 300°C. Figure 5 shows the TGA trace for the nonsuperconducting  $Q$  and  $S$  samples when annealed in  $\text{N}_2$  (a), cooled in  $\text{N}_2$  and reannealed in (b), oxygen and finally cooled in oxygen and reannealed in (c) nitrogen. The difference in  $Q$  and  $S$  is apparent from the curves in (a). Oxygen removal occurs mainly at  $T=400^\circ\text{C}$  for the quenched sample ( $Q$ ) and for the slowly cooled sample ( $S$ ), the maximum oxygen loss occurs for temperatures above 800°C. The total amount of oxygen loss is about 5% smaller for the  $Q$  sample than for the  $S$  sample. After the first nitrogen annealing, the  $Q$  and  $S$  samples behave identically whether reannealed under oxygen [curves in (b)] or nitrogen [curves in (c)], and the TGA traces are similar to those obtained on single crystals.<sup>7</sup> The difference between  $Q$  and  $S$ , with respect to the oxygen removal during the first reducing step, suggests that the excess oxygen in the  $Q$  sample is more mobile and can escape from the sample at a lower temperature than that in the  $S$  sample. We propose that at high temperatures, because of entropic effects, one favors oxygen disorder. Thus, perhaps in the  $S$  samples these oxygens order at some temperature below 1100°C (possibly forming a superlattice that should be observed at room temperature), so that their mobility is reduced. Evidence for such a superlattice has been detected by transmission electron microscopy on a slowly cooled Ce-doped sample<sup>7</sup> or F-doped sample.<sup>13</sup> In contrast, in the  $Q$  samples, which are cooled too fast for this order to develop, the oxygens remain disordered and more mobile [no superlattice was detected by transverse-

TABLE I. Lattice parameters of  $\text{La}_{1.08}\text{Dy}_{0.72}\text{Sr}_{0.2}\text{CuO}_{4-x}\text{F}_x$  ( $x=0-0.35$ ) series.

Compounds	$a$ (Å)	$c$ (Å)	$V$ (Å <sup>3</sup> )
$x=0$	$3.8487 \pm 0.0008$	$12.5310 \pm 0.0030$	$185.6160 \pm 0.0873$
$x=0.1$	$3.8483 \pm 0.0010$	$12.5229 \pm 0.0039$	$185.4569 \pm 0.1141$
$x=0.2$	$3.8491 \pm 0.0013$	$12.5230 \pm 0.0057$	$185.5376 \pm 0.1511$
$x=0.35$	$3.8508 \pm 0.0011$	$12.5044 \pm 0.0043$	$185.6222 \pm 0.1247$

electromagnetic mode on quenched samples]. After the removal of the mobile oxygens from the structure during the first reducing treatment, the samples behave identically with respect to their ability to insert or deinsert oxygen (the anomaly at 400°C disappears in both the *Q* and *S* samples). This feature is not only typical of the  $\text{Nd}_{1.85}\text{Ce}_{0.15}\text{CuO}_4$  sample, but it is also observed in all the other  $R_{1.85-x}R'_xM_{0.15}\text{CuO}_2$  samples investigated. Figures 5(d) and 5(e) show the TGA data for the  $\text{Eu}_{1.85}\text{Ce}_{0.15}\text{CuO}_2$  and  $\text{Eu}_{0.95}\text{La}_{0.9}\text{Ce}_{0.15}\text{CuO}_2$  compounds, respectively. As before, after the first oxygen removal under  $\text{N}_2$  the step present at 400°C disappears on subsequent oxygen removal, and further oxygen loss occurs only for temperatures greater than 800°C. The

weight gain and loss then becomes identical. We have already discussed that the drop in weight at 400°C in Fig. 5(a) could be from disordered oxygen in interstitial sites and the drop at 800°C from ordered oxygen in the same sites. The small dip at 400°C in Fig. 7 may indicate that the ordering is not complete in samples cooled in air from 1100°C.

To investigate the effect of cooling rate on  $T_c$ , the non-superconducting pellets *Q* and *S* were each broken into two pieces. All four pieces were annealed under nitrogen at 900°C for 10 h and either quenched from 900°C or slowly cooled (8 h). The resulting samples are denoted *QQ*, *QS*, *SQ*, and *SS* where *QQ* stands for a sample that has been quenched after both step 1 (treatments at 1100°C) and step 2 (reducing treatment at 900°C), whereas *QS* stands for the pellet that has been quenched after step 1 and slowly cooled after step 2, and vice versa for the *SQ* and *SS* samples. Figure 6 shows the resistive temperature dependence for these four samples. The samples *QQ*, *QS*, *SQ*, and *SS* superconduct with onset temperatures 23, 25.3, 23.2, and 22.5 K and zero-resistance temperatures of 16.5, 19.5, 19, and 18 K, respectively. The room-temperature resistivity values increase in going from the *SS* to the *QQ* samples (uncertainty in the relative resistivity values are less than 10%). The temperature dependence of the resistivity is semiconductinglike for the samples that were quenched in step 1 (*QQ* and *QS*), whereas it is flat or even slightly metalliclike for  $T > 150$  K for samples that were slowly cooled in step 1 (*SQ* and *SS*). Note that the *QQ* and *SQ* samples look just like *QS* and *SS*, respectively, but shifted to higher resistivity. These similarities in temperature dependence suggest that the first step (at 1100°C) changes

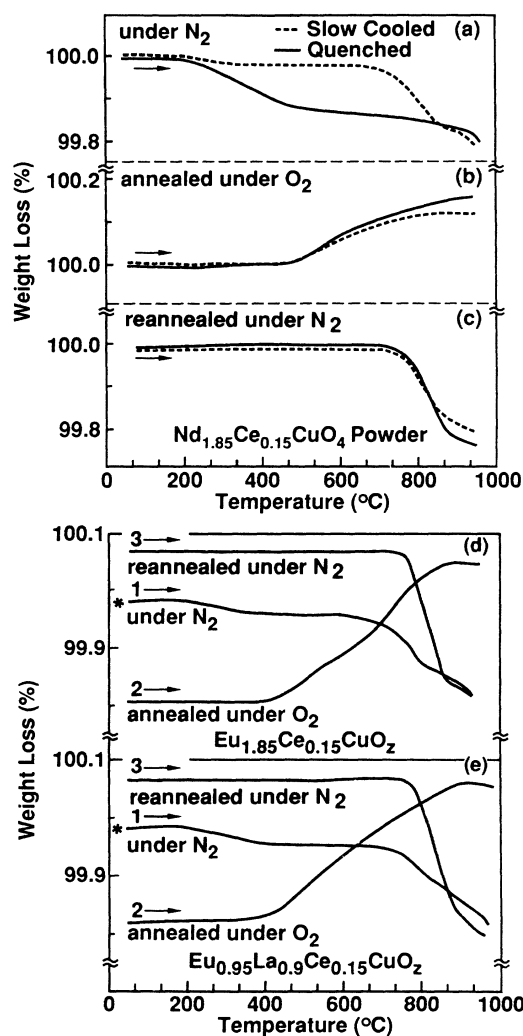


FIG. 5. Effect of processing (cooling rate and ambient) on the oxygen content for  $\text{Nd}_{1.85}\text{Ce}_{0.15}\text{CuO}_2$ , (a) sample annealed under nitrogen, (b) sample annealed under oxygen after quenching, (c) sample reannealed under nitrogen after quenching. The solid curve is for a sample quenching from 1100°C in air, and the dashed curve is the slowly cooled sample. In (d) and (e) the TGA curves for  $\text{Eu}_{1.85}\text{Ce}_{0.15}\text{CuO}_2$  and  $\text{Eu}_{0.95}\text{La}_{0.9}\text{Ce}_{0.15}\text{CuO}_2$ , respectively, are shown. The samples were heated in  $\text{N}_2$  (1), annealed in  $\text{O}_2$  (2), and finally reannealed in  $\text{N}_2$  (3).

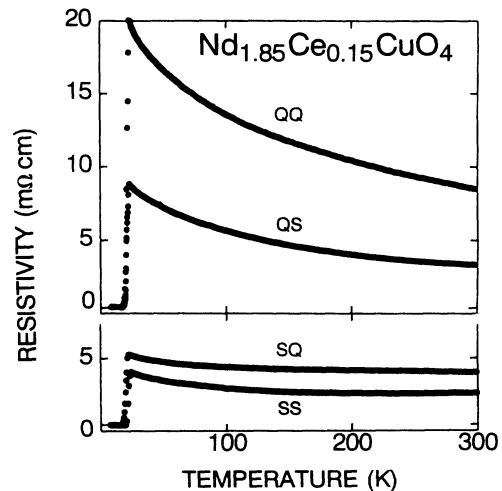


FIG. 6. Effect of cooling rate on the resistivity on  $\text{Nd}_{1.85}\text{Ce}_{0.15}\text{CuO}_4$ . The notation is *Q* for quench and *S* for slow cool. The first letter represents the cooling rate from 1100°C and the second, the cooling rate after anneal at 900°C. Note that the processing from high-temperature determines the shape of the resistivity temperature dependence and the processing from 900°C the room-temperature value.

TABLE II. TGA results for the  $\text{Nd}_{2-x}\text{Ce}_x\text{CuO}_z$  and  $\text{Nd}_{1.55}\text{R}_{0.3}\text{M}_{0.15}\text{CuO}_z$  series. ( $R' = \text{La}, \text{Y}$ ;  $M = \text{Ce}, \text{Th}$ ).  $\text{H}_2$  reduction data taken up to  $870^\circ\text{C}$ .  $\text{N}_2$  and  $\text{O}_2$  data taken up to  $950^\circ\text{C}$ .

Compounds	Oxygen content ( $y$ ) after step ( $a$ )	Oxygen content ( $y$ ) after step ( $b$ )	Change in oxygen $\Delta Y$ between step ( $a$ ) and step ( $b$ )	$[\text{O}]_{\text{N}_2}$	$[\text{O}]_{\text{O}_2}$
$\text{Nd}_2\text{CuO}_z$	4.1097	4.044	0.066	0.1144	0.068
$\text{Nd}_{1.95}\text{Ce}_{0.05}\text{CuO}_z$	4.1228	4.028	0.095	0.91	0.0364
$\text{Nd}_{1.9}\text{Ce}_{0.1}\text{CuO}_z$	4.065	4.0136	0.0514	0.1116	0.0519
$\text{Nd}_{1.85}\text{Ce}_{0.15}\text{CuO}_z$	4.032	3.991	0.041	0.0908	0.0415
$\text{Nd}_{1.8}\text{Ce}_{0.2}\text{CuO}_z$	4.031	3.977	0.054	0.0778	0.0389
$\text{Nd}_{1.55}\text{La}_{0.3}\text{Ce}_{0.15}\text{CuO}_z$	4.001	3.974	0.027	0.0595	0.0440
$\text{Nd}_{1.55}\text{Y}_{0.3}\text{Ce}_{0.15}\text{CuO}_z$	4.033	3.989	0.044	0.0573	0.0174
$\text{Nd}_{1.55}\text{La}_{0.3}\text{Th}_{0.15}\text{CuO}_z$	4.034	3.998	0.036	0.0615	0.0321

the term that controls the temperature dependence of the resistivity, whereas the second step (at  $900^\circ\text{C}$ ), changes a constant term in the resistivity. Resistivity measurements are sensitive to disorder with resistivity values increasing with increasing structural disorder. Thus our data suggests that there are two types of disorder (disorder may be cationic or anionic including phases with different oxygen ordering) produced by the different treatment and that the degree of structural disorder is greater for the  $QQ$  than for the  $SS$  samples. This is in agreement with our model derived from the TGA results; that quenching favors structural disorder. From the TGA measurements, one would expect that superconductivity could be induced in a quenched sample by annealing it under nitrogen at  $600^\circ\text{C}$ . However, annealing a quenched sample at  $600^\circ\text{C}$  for 12 h did not produce superconductivity. We find that independent of the cooling rate after the reducing treatment, superconductivity can only be induced in these materials for reducing temperatures greater than  $850^\circ\text{C}$ . Similarly, we find that superconductivity can only be destroyed by reannealing them under oxygen at  $T > 800^\circ\text{C}$ . Thus, like the La-Sr-Cu-O system, the changes in oxygen and  $T_c$  in these  $T'$  materials are reversible.

Table II displays the total oxygen content, as deduced by TGA measurements using a reducing atmosphere (less than 5%  $\text{H}_2$  in argon), for several as-grown and nitrogen annealed members of the  $\text{Nd}_{2-y}\text{Ce}_y\text{CuO}_z$  and  $\text{Nd}_{2-x}\text{La}_x\text{M}_{0.15}\text{CuO}_z$  series ( $M = \text{Ce}, \text{Th}$ ). Using this technique, an accurate determination of the oxygen content requires a perfect knowledge of the reduced species. For Th, the only reduced species is  $\text{ThO}_2$ . In contrast, for cerium oxide the reduced species  $\text{CeO}_{2-x}$  has stoichiometries that can vary over a wide range of  $x$  (0 to 0.5). Therefore, pure  $\text{CeO}_2$  was reduced under similar conditions as the as-grown material and the reduced species was found to be  $\text{Ce}_2\text{O}_3$ . Thus, we were able to deduce  $z$  for the Ce-doped samples with an accuracy of about 0.5%. Independent of the Ce content, the oxygen content ( $z$ ) per formula unit  $\text{Nd}_{2-y}\text{Ce}_y\text{CuO}_z$  is always greater than 4 (i.e., interstitial oxygens) for the as-grown samples, but decreases with increasing Ce concentration ( $y$ ). In the ideal  $T'$  structure the oxygen apical positions (i.e., oxygen above and below the Cu) are not occupied.

These results suggest a deviation from the  $T'$  structure in that the extra oxygens [determined by both TGA analysis (as earlier) or by chemical titration<sup>14</sup>] may sit on the apical  $4d$  sites. In the following, we will consider that three types of oxygen (oxygen in the  $\text{CuO}_2$  plane, fluorite type, and apical) exist in the  $\text{Nd}_{2-y}\text{Ce}_y\text{CuO}_4$  compounds. Annealing under nitrogen at  $900^\circ\text{C}$  lowers the oxygen content per formula unit, and for the compound with a Ce content of 0.15, the oxygen content becomes lower than 4 (i.e., no extra oxygen). It might be purely a coincidence, but it is for this Ce concentration that the compound becomes superconducting (we stress that caution must be exercised in interpreting these results, since our maximum accuracy in determining the oxygen content is  $\pm 0.5\%$ ). Quite interesting also is the  $\Delta z$  decreases with increasing Ce concentration. In other words, this indicates that the insertion of Ce reduces the ability of these materials to reversibly change oxygen stoichiometry.

To determine how the reversibility of oxygen content varies with Ce content in the  $\text{Nd}_{2-y}\text{Ce}_y\text{CuO}_z$  series, or with the  $R/R'$  ratio within the  $\text{R}_{2-x-y}\text{R}'_y\text{Ce}_{0.15}\text{CuO}_z$  series, we monitored the weight loss or gain of the sample when heated to  $900^\circ\text{C}$  at a rate of  $5^\circ\text{C}/\text{min}$  in a nitrogen ambient [step ( $a$ )], quenched in nitrogen, and reannealed in oxygen to  $950^\circ\text{C}$  at a rate of  $5^\circ\text{C}/\text{min}$  [step ( $b$ )], respectively. The weight loss during step ( $a$ ) or gain during step ( $b$ ) is summarized in Table II for several members of the  $\text{Nd}_{2-y}\text{Ce}_y\text{CuO}_z$  series. Note that the weight loss is always greater than the weight gain, suggesting a slight loss of one element (not yet determined) when the material is heated under nitrogen. Also, the obtained values for the uptake of oxygen agree well with the  $\Delta z$  value, determined previously.

Figures 7(a) and 7(b) only show the TGA traces for the as grown  $\text{Nd}_{2-y}\text{Ce}_y\text{CuO}_z$  and several  $\text{Eu}_{2-x-y}\text{La}_x\text{Ce}_y\text{CuO}_z$  phases, respectively, when annealed under  $\text{N}_2$ . The typical TGA curve can be divided into three regions: Region I spans from room temperature to about  $760^\circ\text{C}$ , region II is from  $\cong 760$  to  $\cong 950^\circ\text{C}$ , and region III is above  $\cong 950^\circ\text{C}$  (data not completely shown). The amplitude of weight loss in oxygen through these regions changes with both the cerium content and with the  $R/R'$  ratio: Both Figs. 7(a) and 7(b) show that the weight loss in region I decreases as Ce doping in-

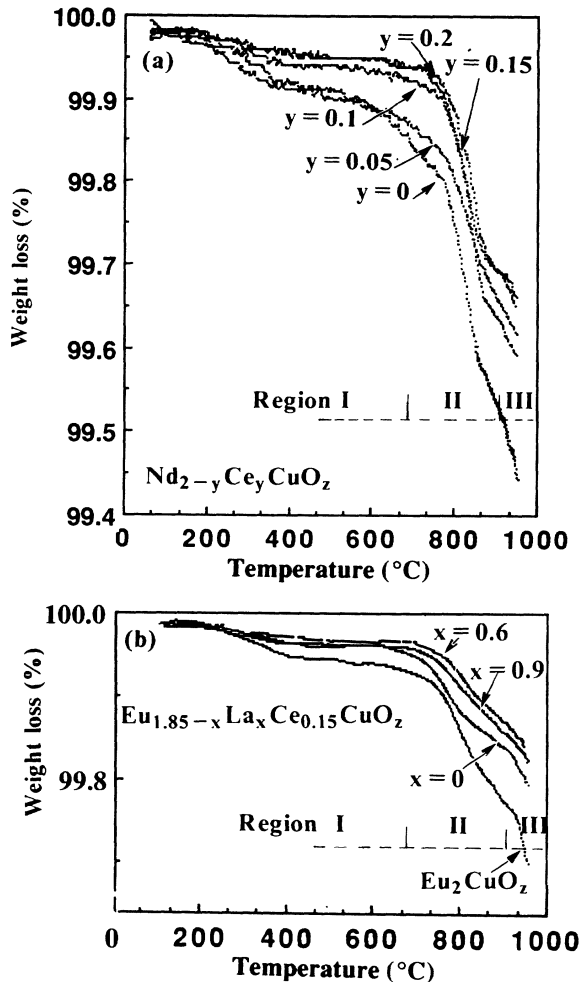


FIG. 7. TGA data for several samples when heated to 850°C at a rate of 5°C/min in a  $N_2$  ambient. In (a) the TGA traces are shown for the  $Nd_{2-y}Ce_yCuO_z$  series and in (b) for the  $Eu_{1.85-x}La_xCe_{0.15}CuO_z$  series.

creases. In contrast, note that upon partial La substitution for Eu, there is no noticeable change in the TGA curves. The weight loss in region II is slightly dependent on the Ce concentration in the  $Nd_{2-y}Ce_yCuO_z$  series, but is not dependent on the type of rare earth substituted for Nd.

The oxygen lost through regions I and II may arise from the interstitial oxygens (i.e., locally ordered or disordered apical oxygen sites). However, one should bear in mind that the  $T'$  phase contains fluorite-type oxygen sandwiched between the rare-earth layers, and that fluorite-type oxides are prone to oxygen defects.<sup>15</sup> Thus it is likely that some of the oxygen loss comes from the fluorite-type layer in the  $T'$  phase. We cannot presently distinguish between these two possibilities, and only further neutron work may resolve this issue (apical versus fluorite-type oxygens) but we can state that it is the oxygen that is removed at 800°C from the structure, which is crucial for superconductivity. The oxygen loss in region III for temperatures greater than 950°C probably comes

from the  $CuO_2$  layer, since we observed that  $T_c$  is suppressed when the compounds are annealed under  $N_2$  at  $T > 950^\circ C$ , and have previously reported that vacancies or disorder in this layer destroy superconductivity. Simultaneously, above 1100°C phase decomposition takes place, as observed by high-temperature x-ray diffraction, discussed in the following. We summarize [Figs. 7(a) and 7(b)] by noting that the total amount of mobile oxygen loss  $\Delta z$  in the  $R_{1.85-x}R'_xCe_yCuO_z$  series is decreasing with increasing the Ce content ( $y$ ) independent of  $R$ , and remains constant  $\Delta z \cong 0.04$  for a fixed Ce content ( $y = 0.15$ ), independent of the  $R/R'$  ratio. We conclude that the role of the nitrogen treatment is twofold: (1) to remove extra oxygens (either "apical" or fluorite type) within the structure and (2) to increase the number of carriers (electrons) through the reduction of  $Cu^{2+}$  to  $Cu^{1+}$ .

Another interesting feature, common to most of the investigated samples, is the change in slope (i.e., kink) in the TGA curves occurring at  $T = 880^\circ C$  during the anneal under nitrogen (i.e., removal of oxygen). Such a slope change may be due to a structural phase transition or a beginning of phase decomposition. To distinguish between these two possibilities, high-temperature x-ray diffraction measurements under nitrogen ambient have been performed on as-grown material. No evidence for such a transition was observed (Fig. 8) up to temperatures of 1100°C. However, note that the spectrum at 1100°C exhibits an extra peak at  $2\theta = 28^\circ$ . This peak, which is still present after cooling the sample to room temperature, is suggestive of a slight amount of phase decomposition. These results clearly indicate the absence of a major structural transition occurring at this temperature, but do not rule out the possibility of an oxygen order-disorder transition that cannot be detected by x rays.

## DISCUSSION

We have shown that within the  $Nd_{2-y}Ce_yCuO_z$  or  $R_{2-x-y}R'_xM_yCuO_y$  ( $R = Nd, Eu$ ;  $R' = La, Y$ ;  $M = Ce, Th$ ) systems there is a subtle and delicate balance between composition, structure and superconducting properties.

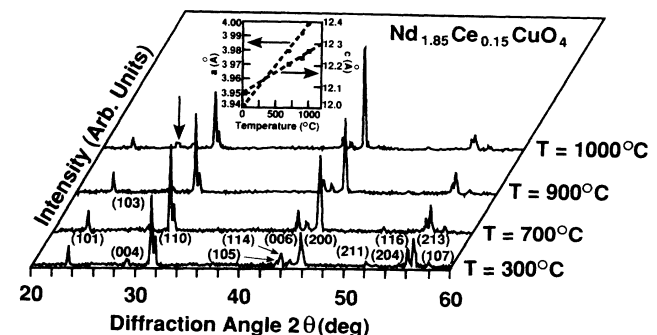


FIG. 8. High-temperature x-ray powder diffraction of  $Nd_{1.85}Ce_{0.15}CuO_4$  under nitrogen ambient. The inset shows the variation of the lattice parameters  $a$  and  $c$  as a function of temperature.

For instance, we showed that for a material with an appropriate cation concentration ( $\text{Nd}_{1.85}\text{Ce}_{0.15}\text{CuO}_2$ ), the superconducting properties can be varied (sharp transition and high  $T_c$  to no  $T_c$  at all), by changing the oxygen content (thereby the Cu oxidation state) through processing conditions (ambient and cooling rate). We also showed that within these new high- $T_c$  oxides, the  $T_c$ 's are independent of whether the rare earth is magnetic or not, which is just what has been found so far for all the high- $T_c$  oxide systems.

In Fig. 9 we compare the variation of the  $a$  and  $c$  lattice parameters for the Sr-doped La system (La-Sr-Cu-O), the Ce-doped Nd system (Nd-Ce-Cu-O) and the La doped Nd system (Nd-La-Cu-O) system. Note that the lattice parameters  $a$  and  $c$  both increase in the La-doped Nd series. Within the same  $T'$  phase when Nd is replaced by Ce, a completely different behavior is observed; an increase in  $a$  and decrease in  $c$  with increasing Ce content. Finally, in the La-Sr-Cu-O system, like for the Ce-doped Nd system  $a$  and  $c$  change in opposite direction. Howev-

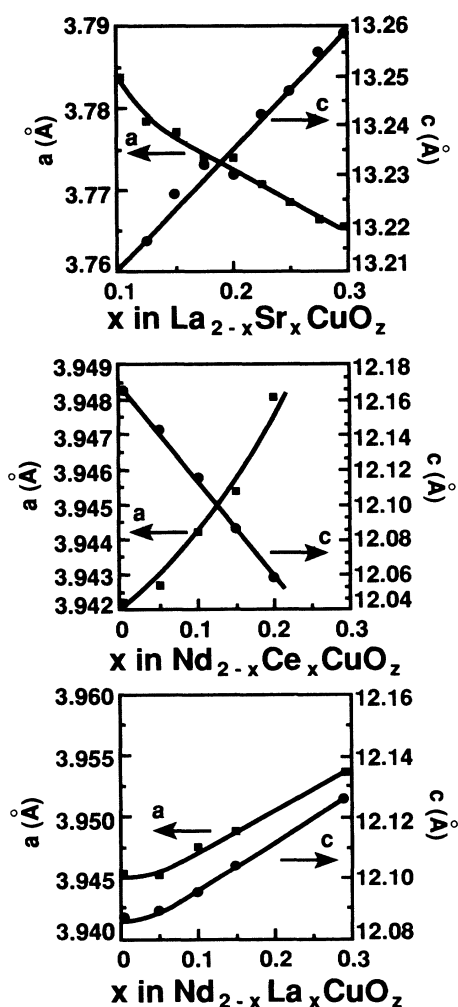


FIG. 9. The variation of the  $a$  and  $c$  lattice parameters are shown as a function of  $x$  for the  $\text{La}_{2-x}\text{Sr}_x\text{CuO}_4$ ,  $\text{Nd}_{2-x}\text{Ce}_x\text{CuO}_4$  and  $\text{Nd}_{2-x}\text{La}_x\text{CuO}_4$  series.

er,  $a$  decreases and  $c$  increases when the trivalent La ions are replaced by divalent Sr ions. The variation of the  $c$  axis in these three systems can simply be understood based on the ionic radius of the dopant versus the substituent. In the  $T$  phase La is located at a nine-coordinated site. The ionic radii of a nine-coordinated  $\text{La}^{3+}$  and  $\text{Sr}^{2+}$  are 1.3 and 1.45 Å, respectively. Thus replacement of La by Sr is expected to increase the  $c$  and  $a$  axis. Only the increase in  $c$  is observed. In the  $T'$  phase, Nd is located at an eight-coordinated site and the ionic radii of eight-coordinated  $\text{Nd}^{3+}$  and  $\text{Ce}^{4+}$  are 1.25 and 1.11 Å, respectively. Thus a shortening of both  $a$  and  $c$  is expected when Nd is replaced by Ce. We find that  $c$  decreases but  $a$  increases. Finally, when Nd is replaced by La in the  $T'$  phase, one should expect an increase of the  $c$  axis and  $a$  axis as observed. Thus based on the ionic radius, one can explain the variation of the  $c$  lattice parameter for the three systems and that of the  $a$  lattice parameter for the La-Nd doped system but not that of  $a$  for the Ce or Sr doped system. A key for understanding these observations is that either Ce or Sr substitution affects the electron or hole concentration, whereas La substitution does not. Thus, this charge transfer might be responsible for the apparently unexpected variation of  $a$  in the Sr-doped La- or Ce-doped Nd systems. Whangbo *et al.*<sup>16</sup> have shown that the Cu—O bonds have antibonding character in the  $\text{CuO}_2$  layer  $x^2-y^2$  bands. The substitution of  $\text{La}^{3+}$  by  $\text{Sr}^{2+}$  corresponds to add a hole or equivalently removing an electron from the  $x^2-y^2$  bands. Thus the removal of an electron from the antibonding band orbital would shorten the in-plane Cu—O bond and first the in-plane Cu—Cu distance (i.e., the  $a$  axis) as experimentally observed. In contrast, doping with Ce corresponds to adding electrons into the antibonding band orbital and thereby lengthening the in-plane Cu—O bond and the Cu—Cu distance as observed. Therefore, the variation of the lattice parameters is quite consistent with the fact that the  $T$  phase is doped by holes ( $p$  type) and that the  $T'$  phase is doped by electrons ( $n$  type).

In the La-Sr-Cu-O system, superconductivity can be achieved either by divalent dopant or oxygen uptake and  $T_c$  is maximum when the formal valence of  $\text{Cu}^{3+}$  (i.e., holes) is close to 2.15. For the Nd-Ce-Cu-O system, Ce doping and oxygen removal (both of which donate electrons to the  $\text{CuO}_2$  layers) are required to promote superconductivity. If there is a critical electron concentration to induce superconductivity it is puzzling why this limit cannot be achieved by further increasing Ce doping only. We have tried, but no superconductivity is observed, without nitrogen reduction, to the limit of Ce solubility ( $\cong 0.2$ ). This illustrates the crucial role of the annealing treatment that removes some oxygen and thereby increases the number of carriers to reach the threshold carrier concentration. TGA analysis has shown, in agreement with the work of Moran *et al.*,<sup>14</sup> that independent of the Ce content the oxygen content in the as-grown material is always greater than four. We have suggested that these extra oxygens occupy the  $4d$  positions (i.e., apical positions). Upon nitrogen reduction, the extra oxygens are partially removed, and according to our data the Ce-doped Nd compound becomes superconductor when



the formal valence of Cu is 1.85 (i.e., 0.15 electrons/Cu), which occurs when the oxygen content becomes lower than four. It is interesting to recall that within the La-Sr-Cu-O system a maximum in  $T_c$  was found for a formal valence of 2.15 for Cu (i.e., 0.15 holes). The accuracy of the TGA measurements is not sufficient to speculate whether or not the presence of apical oxygens is crucial for superconductivity. Future neutron studies should clarify this point.

For La-Sr-Cu-O, the reversible removal of 0.03 oxygen atoms per formula unit occurs in one step at temperatures close to 500°C. For the Nd system the amount of mobile oxygen is similar (0.04 per formula unit) but its removal occurs at higher temperatures (800°C). In both systems the changes in oxygen content and  $T_c$  are reversible.

For all the copper oxide superconductors, a correlation between  $T_c$  and the in-plane Cu-O distance was proposed.<sup>17</sup> For instance, within the La-Sr-Cu-O system there is an optimum bond length (1.888 Å) for which  $T_c$  is maximum<sup>17</sup> and this optimum bond length changes by slightly affecting the structure (i.e., by replacing Sr by Ba or Ca). In Nd-Ce-Cu-O system we found that a similar correlation exists, and clearly shown for the Eu system that there is a critical distance of about 1.95 Å at which  $T_c$  is optimum (16 K). Away from this optimum length,  $T_c$  is decreased. This again suggests the close similarity between the *n*-type and *p*-type and superconductors. In the  $\text{Eu}_{1.85-x}\text{La}_x\text{Ce}_{0.15}\text{CuO}_4$  system, substitution of  $\text{La}^{3+}$  for  $\text{Eu}^{3+}$  does not change the electron concentration, nevertheless its  $T_c$  versus Cu-Cu correlation shows a maximum. The only thing that make sense is that the Cu—O bond strength changes as a function of *x*, as pointed out by Whangbo *et al.*,<sup>17</sup> for the old copper oxide superconductors. We have shown that the *a* and *c* parameters are almost perfectly correlated so that there is a correlation between  $T_c$  and *c*, but this is just a byproduct

of the in-plane Cu-Cu distance correlation. The replacement of Eu by larger ions such as La can, to a certain extent, be viewed as a chemical pressure effect. Thus one would expect hydrostatic pressure to lead to the same effect. In fact recent studies<sup>18</sup> on the pressure dependence of  $T_c$  for several *T'* phases  $M_{1.85}\text{Ce}_{0.15}\text{CuO}_4$  have shown that a maximum in  $T_c$  is observed with increasing pressure for  $\text{Eu}_{1.85}\text{Ce}_{0.15}\text{CuO}_4$ . By increasing the pressure the Cu-O distance (i.e., half of Cu-Cu distance) is changed, and at a certain pressure its bond strength reaches the critical value, thereby leading to a maximum  $T_c$ .

The optimum bond distance for  $T_c$  in the La-Sr-Cu-O and Nd-Ce-Cu-O systems are 1.88 and 1.95 Å, respectively. Thus one might expect for compounds of the *T* or *T'* phase, with Cu-O distances close to the critical values, to exhibit superconductivity if one could find a chemical substitution which will optimize the in-plane Cu—O bond length. In this respect, the  $\text{Gd}_2\text{CuO}_4$  system which has a Cu-O distance close to the optimal one is an interesting candidate. Experiments are presently in progress.

From this study it appears that the *n*- or *p*-type systems behave similarly from a chemical point of view. The only difference is that the nature of the carriers is different (electrons and not holes). The sign of the Hall coefficient,  $R_H$ , which so far has been found to be extremely sample sensitive,<sup>7,19</sup> with either positive or negative values, still raises some questions. Only better materials will help in solving this issue.

#### ACKNOWLEDGMENTS

We wish to thank B. G. Bagley, J. Barner, P. F. Miceli, R. Ramesh, J. M. Rowell, J. H. Wernick, and M.-H. Whangbo for valuable discussions.

<sup>1</sup>J. G. Bednorz and K. A. Muller, *Z. Phys. B* **64**, 189 (1986).  
<sup>2</sup>Y. Tokura, H. Takagi, and S. Uchida, *Nature* **337**, 345 (1989).  
<sup>3</sup>E. Takayama-Muromachi, Y. Matsui, Y. Uchida, F. Izumi, M. Onoda, and K. Kato, *Jpn. J. Appl. Phys.* **27**, L2282 (1988).  
<sup>4</sup>S.-W. Cheong, Z. Fisk, J. D. Thompson, and R. B. Schwarz, *Physica* **162-164C**, 1681 (1989).  
<sup>5</sup>H. Fjellvag, P. Karen, and A. Kjekshus, *Acta Chem. Scand. A* **42**, 144 (1988).  
<sup>6</sup>A. C. W. P. James, S. M. Zahurak, and D. W. Murphy, *Nature* **338**, 240 (1989).  
<sup>7</sup>J. M. Tarascon, E. Wang, L. H. Greene, R. Ramesh, B. G. Bagley, G. W. Hull, P. F. Micelli, Z. Z. Wang, D. Brawner, and N. P. Ong, *Proceedings of the  $M_2S$ -HTSC Conference, Stanford, 1989* [*Physica C* (to be published)].  
<sup>8</sup>J.-M. Tarascon, L. H. Greene, W. R. McKinnon, G. W. Hull, and T. H. Geballe, *Science* **13**, 1373 (1987).  
<sup>9</sup>H. Takagi, S. Uchida, and Y. Tokura, *Phys. Rev. Lett.* **62**, 1197 (1989).  
<sup>10</sup>J.-M. Tarascon, L. H. Greene, W. R. McKinnon, and G. W. Hull, *Solid State Commun.* **63**, 499 (1987).  
<sup>11</sup>J. T. Markert, E. A. Early, T. Bjornholm, S. Ghamaty, B. W.

Lee, J. J. Neumeier, R. D. Price, C. L. Seaman, and M. B. Maple, *Physica C* **158**, 178 (1989).  
<sup>12</sup>J. T. Markert and B. Maple, *Solid State Commun.* **70**, 145 (1989).  
<sup>13</sup>C. H. Chen, D. J. Werder, A. C. W. P. James, D. W. Murphy, S. Zahurak, R. M. Fleming, B. Batlogg, and L. F. Schemeyer, *Physica* **160C**, 375 (1989).  
<sup>14</sup>E. Moran, A. I. Nazzal, T. C. Huang, and J. B. Torrance, *Physica* **160C**, 30 (1989).  
<sup>15</sup>L. E. Roberts, *Nonstoichiometric Compounds*, edited by R. F. Gould (American Chemical Society, Washington, D.C., 1963), pp. 66–73.  
<sup>16</sup>M.-H. Whangbo, M. Evain, M. Beno, and J. M. Williams, *Inorg. Chem.* **26**, 1829 (1987).  
<sup>17</sup>M.-H. Whangbo, D. B. Kang, and C. C. Torardi, *Physica C* **158**, 371 (1989).  
<sup>18</sup>B. Maple *et al.* (unpublished).  
<sup>19</sup>H. Takagi, Y. Tokura, and S. Uchida, *Proceedings of the ( $M_2S$ -HTSC Conference, Stanford, 1989* [*Physica C* (to be published)]).